Image-based fracture mechanics of cortical bone during *in situ* SRµCT three-point bending

Marcin Sikorski[1a], Sebastian Levin[2], Lorna Sinclair[3], Yuhang Chen[1], Christina Reinhard[3], Uwe Wolfram[2], Marta Peña Fernández[1]

[1]Heriot-Watt University, UK, [2]Clausthal University of Technology, Germany, [3]The University of Manchester at Harwell, Diamond Light Source, UK

[a]mms10@hw.ac.uk

Introduction

Bone fractures arising from changes in bone tissue microstructure and composition due to ageing or disease impose a major global healthcare burden [1]. A deeper understanding of the underlying failure mechanisms in relation to bone microstructure may help to develop better diagnoses and therapies. The combination of X-ray synchrotron radiation micro-computed tomography (SRµCT) with *in situ* mechanical tests and digital volume correlation (DVC) enables high-resolution imaging of bone microstructure and full-field quantification of displacements and strain fields, which can be used for analysis of bone fracture toughness properties and microdamage evolution in 3D [2]. However, DVC accuracy is highly sensitive to image quality and requires effective denoising. Self-supervised deep learning methods, such as Noise2Inverse (N2I), have shown promise for improving SRµCT image quality without clean reference data [3]. Therefore, this study aims to: (i) assess the impact of N2I noise reduction on DVC measurements, (ii) measure full-field 3D displacements and strains in cortical bone under mechanical loading using DVC, and (iii) track microcrack initiation and propagation within the tissue.

Materials and methods

Cortical bone bending specimens (11 × 2 × 1 mm³) were machined from ovine femur in longitudinal and transverse orientations (n = 6 per orientation) and notched to introduce an initial crack. In situ three-point bending tests were performed at beamline I13-2 (Diamond Light Source, UK) using a Deben CT500 loading stage (3 mm diameter pins, 8 mm span), with specimens immersed in saline solution (PBS) to simulate physiological conditions. A polychromatic X-ray beam (6–25 keV, 200 mA, 2 × 2 mm, Pt mirror 4.6 mrad) was used with Al and Fe filters (2 mm and 50 µm). Specimens were loaded in steps of 2 N (Figure 1a), and following mechanical relaxation at each load stage, a tomographic scan (0.81 µm voxel size, 2250 projections, 0.2 s/projection) was acquired (Figure 1c).

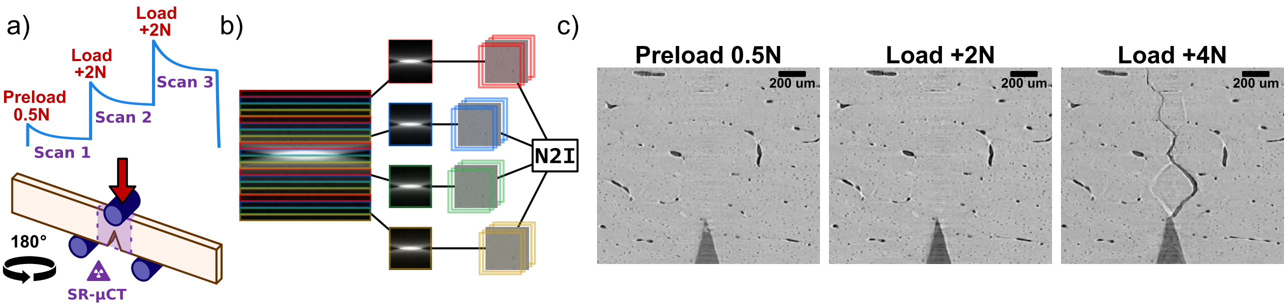

Figure 1. a) Schematic of the in situ SRµCT three-point bending setup with the loading protocol and tomographic acquisition at each load step. b) Noise2Inverse (N2I) denoising pipeline, in which sinograms are split, independently reconstructed, and used to train denoising network. c) Representative images showing crack initiation and propagation under incremental load steps.

Tomographic reconstruction (2560 × 2560 × 2110) was performed by filtered back-projection (FBP) implemented in Savu software [4] from which VOIs (1700 × 1550 × 1500) were extracted. Reconstructions were subsequently denoised using Noise2Inverse (N2I) [3] approach implemented with Mixed-Scale Dense (MSD) network, trained on randomly subsampled patches (1300 × 1300, 500 slices per split) drawn from 5 scans and validated against a held-out scan. The effect of N2I denoising was evaluated at two projection-splitting levels (k= 2, k = 4) and compared against unfiltered and 3D Gaussian-filtered (σ = 2) images.

Full-field 3D displacements and strains were quantified using DVC (DaVis 11.3 LaVision) with rigid-body motion correction. Measurement uncertainty was assessed by correlating two repeated zero-load scans, from which representative VOIs (1000×1000×1300 voxels) were extracted, where any displacement measured reflects registration error [5]. DVC parameters were optimised using 4 multipass schemes [5] with final subvolume sizes ranging from 48 to 24 voxels. Displacement uncertainty was reported as the standard deviation of each displacement component, while strain accuracy and precision were quantified as mean absolute error (MAER) across all six strain components and its standard deviation (SDER), respectively [5].

Results

Denoising had a strong effect on DVC performance across all subvolume sizes and both orientations (Figure 2). Mean correlation scores were 0.19–0.21 for unfiltered reconstructions, 0.79–0.84 for 3D Gaussian-filtered, and 0.93–0.95 for N2I-denoised volumes. For N2I-denoised scans, MAER decreased from 1800–2200 to 285–325 με (k = 2) and from 940–1100 to 285–320 με (k = 4), with max. displacement std. deviations reduced from 0.149–0.154 and 0.096–0.098 to 0.053–0.059 μm respectively. The 3D Gaussian filter showed a similar trend (MAER: 1100–2040 to 305–538 με; max. displacement uncertainty: 0.096–0.168 to 0.051–0.091 μm) but with a larger spread between orientations. N2I (k = 4) was selected for subsequent analysis based on smaller differences between orientations, with a final subvolume size of 40 voxels (MAER: 375–449 με, SDER: 162–192 με, max. displacement std. dev.: 0.062–0.066 μm).

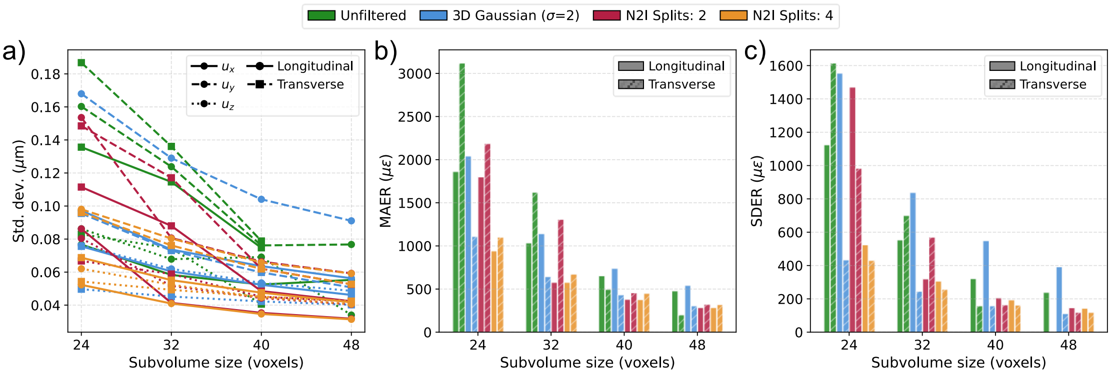

Figure 2. DVC uncertainty results: a) displacement errors, b) strain accuracy (MAER) c) strain precision (SDER).

The DVC analysis of the transverse specimen under 2 N load (Figure 3a) provided 3D displacement and strain fields. The x-displacement field (Figure 3b) exhibited a clear antisymmetric pattern about the notch axis reaching up to ±0.6 μm at the lateral edges of the field of view. The maximum principal strain field (Figure 3c) at the sample midplane showed localised concentrations near the crack tip reaching approximately 8000 με.

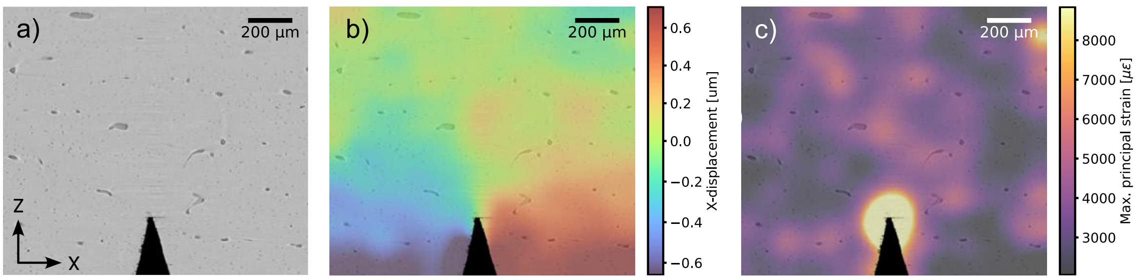

Figure 3. DVC results at the midplane of a transverse sample under 2 N load. a) SRμCT reconstruction (loaded stage). b) X-displacement field. c) Maximum principal strain field

Discussion and future work

The implemented N2I deep learning denoising substantially improved DVC measurement quality relative to conventional filtering. The superior performance of N2I over 3D Gaussian filtering reflects its ability to suppress noise while preserving microstructural features without blurring effect [3]. This enables their accurate tracking and reduces uncertainty in obtained displacement and strain measurements, allowing for more precise characterisation of crack-tip deformation at the micrometre scale in cortical bone. The antisymmetric x-displacement pattern and localised maximum principal strain concentrations near the notch tip are consistent with mode I crack opening [6] and localised plastic zone, due to stress concentrations driving microcracking ahead of the notch [7]. Future work will extend the analysis to the full loading sequence and all samples to track the evolution of strain fields with increasing load prior to failure. Crack-opening displacements will be measured and compared between orientations to quantify anisotropy in cortical bone fracture toughness.

References

[1] M. J. Mirzaali et al., 'Mechanical properties of cortical bone and their relationships with age, gender, composition and microindentation properties in the elderly', Bone, vol. 93, pp. 196–211, Dec. 2016, doi: 10.1016/j.bone.2015.11.018.
[2] M. Peña Fernández et al., 'In situ synchrotron radiation μCT indentation of cortical bone: Anisotropic crack propagation, local deformation, and fracture', Acta Biomater., vol. 167, pp. 83–99, Sep. 2023, doi: 10.1016/j.actbio.2023.04.038.
[3] A. A. Hendriksen et al., 'Noise2Inverse: Self-Supervised Deep Convolutional Denoising for Tomography', IEEE Trans. Comput. Imaging, vol. 6, pp. 1320–1335, 2020, doi: 10.1109/TCI.2020.3019647.
[4] N. Wadeson and M. Basham, 'Savu: A Python-based, MPI Framework for Simultaneous Processing of Multiple, N-dimensional, Large Tomography Datasets'.
[5] M. Peña Fernández et al., 'Optimization of digital volume correlation computation in SR-microCT images of trabecular bone and bone-biomaterial systems', J. Microsc., vol. 272, no. 3, pp. 213–228, Dec. 2018, doi: 10.1111/jmi.12745.
[6] R. O. Ritchie et al., 'A fracture mechanics and mechanistic approach to the failure of cortical bone', Fatigue Fract. Eng. Mater. Struct., vol. 28, no. 4, pp. 345–371, Apr. 2005, doi: 10.1111/j.1460-2695.2005.00878.x.
[7] R. O. Ritchie et al., 'Plasticity and toughness in bone', *Phys. Today*, vol. 62, no. 6, pp. 41–47, Jun. 2009, doi: 10.1063/1.3156332.

Acknowledgments

We thank Dr Sam McPhee, Dr Leonard Turpin and Dr Kaz Wanelik for support during beamtime at Diamond Light Source (MG35848).